J. Indian Chem. Soc.,
Vol. 94, July 2017, pp. 699-706

A novel imidazolyl appended quinoline-hydrazide Schiff base fluorescent chemosensor for precise identification of Zn^{II}

Rakesh Purkait and Chittaranjan Sinha*

Department of Chemistry, Jadavpur University, Kolkata-700 032, India

E-mail : c_r_sinha@yahoo.com

Manuscript received 19 May 2017, accepted 24 May 2017

Abstract : (*E*)-*N*′-((1*H*-imidazol-2-yl)methylene)quinoline-2-carbohydrazide (H_2L) is synthesized by the reaction of acid hydrazide and carbaldehyde. The probe has been characterized by spectroscopic data (FT-IR, UV-Vis, ^1H NMR) and is weakly emissive. The H_2L selectively binds Zn^{2+} and upon irradiation at 331 nm in presence of large number of cations shows high intense emission (λ_{em}, 575 nm) and serves as a "turn-on" fluorescence chemosensor. The limit of detection (LOD) for Zn^{2+} is 0.36 μM. Formation of the 1 : 1 metal-to-ligand complex has been ascertained by Mass spectra and Job's plot.

Keywords : Quinoline-carbohydrazide, Zn^{2+}-sensor, LOD 0.36 μM, 1 : 1 complex, spectral characterization.

Introduction

Elements are essential for the origination, growth and reproduction of living bodies. About 98% of the body mass of man is made up of nine nonmetallic elements[1]. Transition metals present in trace and some are in ultratrace level in human body[2]. Elements such as iron, zinc, copper etc. are essential components of enzymes and facilitate their conversion to specific end products. Zinc, the second-most abundant (transition) metal following iron in the human body, is an omnipotent metal and the average body content is 2–3 g in an adult[3]. The standard daily requirement of zinc is 15–20 mg/day. Zinc plays an important role in cell proliferation, immunological and psychological functions and in metabolic activity. Plasma zinc levels are decreased in pregnancy, acute myocardial infarction, infections, and malignancies. It is essential for normal spermatogenesis and maturation, functioning of neurotransmitters, development of thymus, epithelialization, taste sensation, and secretion of pancreas and gastric enzymes. The excess "free zinc" may induce pathological diseases such as Alzheimer's and Parkinson's disease[4]. Moreover, excess of zinc in the environment may reduce soil microbial activity, which has phytotoxic effects[5–7]. Thus detection of Zn^{2+} is pressing important for monitoring human health. Exploration of selective and sensitive chemosensor for detection of ions in solution has been of considerable attention with biological and environmental interest[8–14]. In the last two decades, significant number of fluorescent probes have been designed and some have been used successfully in sensing of zinc at ultratrace level. Most of them have been developed based on quinoline[15], bipyridyl[16], coumarine[17], pyrazoline[18], tripyrrins[19], BINOL[20], fluorescein[21], rhodamine[22], fluorophores. Quinoline based fluorophore[15,23] is associated with imine (C=N), amide (-CONH-), sulfonyl derivatives etc.; however, quinoline-hydrazide has not been used for investigating sensor activity. In this work, we have designed and synthesized a hydrazide based imidazole derivative, (*E*)-*N*′-((1*H*-imidazol-2-yl)methylene)quinoline-2-carbohydrazide for the selective and sensitive detection of Zn^{2+} in presence of other commonly available metal ions. The DFT computation of optimized geometry of H_2L and the complex has been used to explain the electronic spectral properties.

Experimental

Materials and methods

Quinaldic acid and imidazole-2-carbaldehyde were purchased from Sigma-Aldrich and quinoline-2-

carbohydrazide was synthesized following the published procedure[24]. All other organic chemicals and inorganic salts were obtained from commercial suppliers Merck and used without further purification. Aqueous solutions were prepared using Milli-Q water (Millipore). Elemental analyses were performed using a Perkin-Elmer 2400 Series-II CHN analyzer, Perkin-Elmer, USA elemental analyzer. UV-Vis spectra were recorded on Perkin-Elmer Lambda 25 spectrophotometer and fluorescence spectra were obtained using a Perkin-Elmer spectrofluorimeter model LS55, FT-IR spectra (KBr disk, 4000–400 cm^{-1}) from a Perkin-Elmer LX-1FTIR spectrophotometer. NMR spectra were obtained on a Bruker (AC) 300 MHz FT-NMR spectrometer using TMS as an internal standard. ESI mass spectra were recorded from a Water HRMS model XEVO-G2QTOF#YCA351 spectrometer. All of the measurements were conducted at room temperature. The fluorescence quantum yield was determined using fluorescein as reference with a known quantum yield, ϕ_R = 0.79 in 0.1 *M* NaOH[25]. The experimental sample and reference were excited at same wavelength, maintaining almost same absorbance and fluorescence were measured. Area of the fluorescence spectra were measured using the software available in the instrument and the quantum yield was calculated by following the formula

$$\phi_S/\phi_R = \left[A_S/A_R\right] \times \left[(\mathrm{Abs})_R/(\mathrm{Abs})_S\right] \times \left[\eta_S^2/\eta_R^2\right]$$

where, η_S and η_R are the fluorescence quantum yield of the samples and reference; A_S and A_R are the respective areas under emission spectra of the sample and reference respectively. $(Abs)_R$, $(Abs)_S$ are the absorbance of sample and reference at the excitation wave length and η_S^2, η_R^2 are the refractive index of the solvent used for the sample and the reference.

Synthesis of probe, H_2L

The condensation of quinoline-2-carbohydrazide (0.187 g, 1.0 mmol) and imidazole-2-carbaldehyde (0.097 g, 1.0 mmol) under stirring condition in dry MeOH (15 ml) for 5 h at room temperature yields a grey precipitate. It was filtered off and washed several times with MeOH and dried in open air. Yield : 88%, m.p. >200 °C (Scheme 1). Microanalytical data : $C_{20}H_{13}N_3O_3$ Calcd. (Found) : C, 63.39 (63.35); H, 4.18 (4.19); N, 26.40 (26.37)%; ^{1}H NMR (300 MHz, DMSO-d_6) : 15.29 (1H, s, imidazole-NH), 12.31 (1H, s, NH), 8.63 (1H, s, imine-H), 8.25–7.99 (2H, m), 7.99–7.85 (2H, m), 7.72 (1H, d, 18Hz), 7.51 (1H, t, 18Hz), 7.26 (1H, d, 15Hz), 7.09 (1H, s) (ESI†, Fig. S1); IR : 3240 cm^{-1} (hydrazide -NH), 1668 cm^{-1} (–C=O), 1539 cm^{-1} (azomethine, -C=N), (ESI†, Fig. S2).

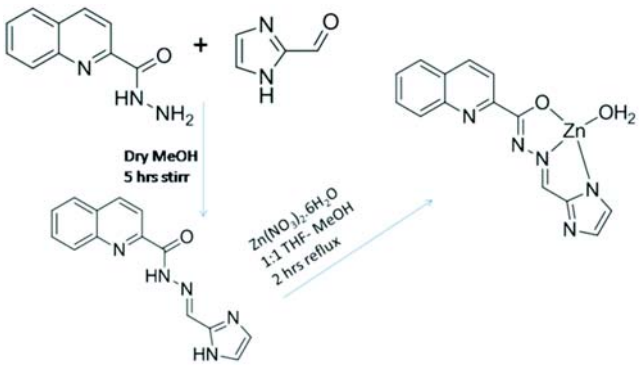

Scheme 1. Synthesis of H_2L and the complex, [ZnL(H_2O)].

Synthesis of [ZnL(H_2O)]

To THF-MeOH (1 : 1, v/v, 10 ml) solution of H_2L (1 mmol, 0.265 g), MeOH solution (10 ml) of $Zn(NO_3)_2.6H_2O$ (0.297 g, 1 mmol) was added and refluxed for 3 h to yield a red precipitate. It was filtered off and washed several times with MeOH and dried in open air. Microanalytical data : Calcd. (%) C, 48.37; H, 3.48; N, 20.14; ^{1}H NMR (300 MHz, DMSO-d_6) : 8.85 (1H), 8.75 (1H), 8.57 (1H), 8.41 (1H), 8.17 (1H), 7.95 (1H), 7.80 (1H), 7.42 (1H), 7.28 (1H), 7.09 (1H) (ESI†, Fig. S3); IR : 3434 cm^{-1} (ν(H_2O)), 1529 cm^{-1} (azomethine, -C=N), (ESI†, Fig. S4).

General method for UV-Vis and fluorescence studies

The probe, H_2L (1.32 mg, 0.001 mmol) was dissolved in THF (5 ml) and 100 μL of H_2L solution diluted using 2 ml THF-MeOH (v/v 1 : 1) containing HEPES buffer (pH 7.2) to make the solution with total volume 2.1 ml. $Zn(NO_3)_2.6H_2O$ (2.97 mg, 0.001 mmol) was dissolved in water (10 ml). The Zn^{2+} so-

lution (100 μL) were transferred to H_2L solution prepared above. This procedure for sample solution preparation also maintained for other cations. After mixing spectra were recorded at room temperature. For fluorescence study excitation wavelength used was 331 nm (excitation slit = 10.0 and emission slit = 10.0).

Theoretical computation

H_2L and [ZnL(H_2O)] were optimized to generate the structures by DFT/B3LYP method using Gaussian 09 software[26,27]. 6-311G basis set was used for C, H, N, O, and LanL2DZ basis set was used as effective potential (ECP) set for Zn. To ensure the optimized geometries represent the local minima, vibrational frequency calculations were performed, and these only yielded positive eigen values. Theoretical UV-Vis spectra were calculated by time-dependent DFT/B3LYP method in methanol using conductor-like polarizable continuum model (CPCM)[28,29]. GAUSSSUM was used to calculate the fractional contributions of various groups to each molecular orbital[30].

Results and discussion

Synthesis and formulation

The condensation of quinoline-2-carbohydrazide and imidazole-2-carbaldehyde synthesised (*E*)-*N*′-((1*H*-imidazol-2-yl)methylene)quinoline-2-carbohydrazide (H_2L) in good yield (88%). It has been characterized by spectroscopic data (FTIR, Mass, NMR; ESI†). Molecular ion peak, $(H_2L+H)^+$ 265.03 (Mwt., 265.27) supports the molecular identity. The broad band at 3240 cm^{-1} refers to ν(hydrazide-NH) and strong stretches at 1668 cm^{-1} and 1609 cm^{-1} are assigned to ν(C=O) and ν(C=N) respectively. The ^1H NMR spectrum of H_2L (300 MHz, DMSO-d_6) demonstrates singlet at 15.29 ppm corresponds to δ(imidazole-NH); hydrazine-NH appears at 12.31 ppm; imine-H (CH=N) appears at δ 8.63 ppm; and aromatic protons appear at 7.0–8.3 ppm. The reaction of H_2L with $Zn(NO_3)_2.6H_2O$ in methanol has isolated mononuclear zinc complex, [ZnL.(H_2O)]. The complex has shown a broad peak at 3434 cm^{-1} corresponds to ν(H_2O) and ν(C=N) is observed at 1592 cm^{-1} which is shifted to lower energy compared to H_2L. Mass spectrum shows molecular ion peak at 368.05 which may be due to $[ZnL(H_2O)+Na]^+$. The absence of δ(hydrazide-NH) and δ(imidazolyl-NH) support ionization of probe and its binding with Zn^{II} during synthesis. All other protons quantitatively appear in the spectrum. Thermal treatment eliminates coordinated H_2O at 112 °C which is supported by elimination of broad stretch at 3434 cm^{-1} in the infrared spectrum. Thus, the structure proposal of probe and the complex (Scheme 1) are established.

UV-Vis spectroscopic studies

The interaction of H_2L with Zn^{2+} has been examined by spectrophotometric titration of H_2L with incremental addition of Zn^{2+} in HEPES buffer (10 mM, pH 7.2) at 25 °C in the same solvent, and has shown absorption enhancement at 383 nm and decrement at 332 nm, with the isosbestic point at 355 nm (Fig. 1) which suggests that the reaction is clean and straightforward. The red-shifting of the bands of H_2L upon Zn^{2+} addition is attributed to expulsion of intramolecular charge transfer (ICT) through the chelation. The change of absorbance is linear until the molar ratio $[Zn^{2+}]$: $[H_2L]$ reaches 1 : 1, and no longer changes with increase in $[Zn^{2+}]$. It suggests that the stoichiometry between H_2L and Zn^{2+} is 1 : 1. To establish the binding stoichiometry of H_2L and Zn^{2+}

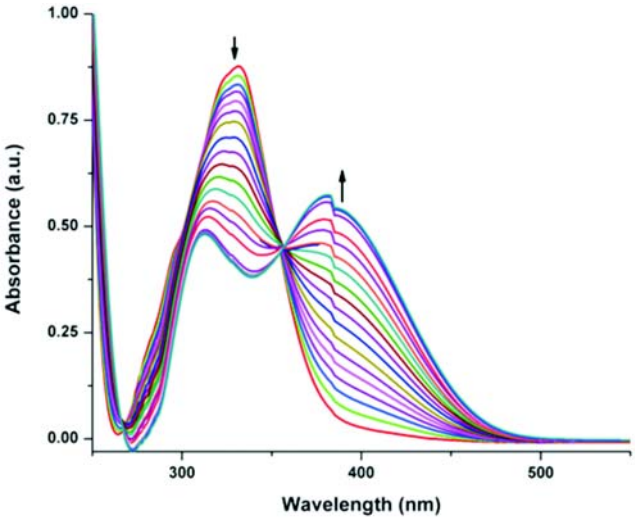

Fig. 1. Change in absorption spectrum of H_2L (50 μM) upon gradual addition of Zn^{2+} ions (5 μM each) in THF-MeOH (v/v 1 : 1) (pH 7.2).

the Job's plot has been generated by plotting absorbance against different mole fractions of Zn^{2+} while volume of solution has remained fixed (Fig. 2) and the molar fraction maxima has been obtained at 0.5 mole fraction, which indeed supports 1 : 1 complex formation of H_2L and Zn^{2+}.

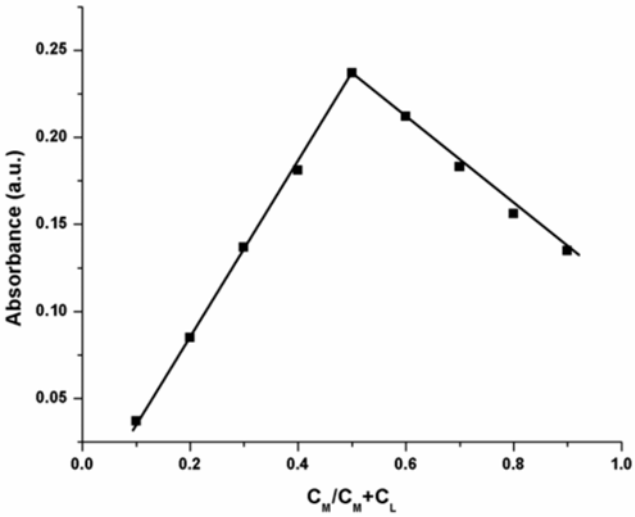

Fig. 2. Job's plot for the reaction between H_2L and Zn^{2+} in THF-methanol (1 : 1, v/v).

Fluorescence sensing for Zn^{2+}

Upon excitation the probe (H_2L) at 331 nm, a weak emission is observed at 500 nm with fluorescence quantum yield (ϕ_{HL}) 0.0021. On addition of Zn^{2+} the emission band is red shifted to 575 nm. The fluorescence emission of H_2L with other cations (Na^+, K^+, Ca^{2+}, Mg^{2+}, Mn^{2+}, Fe^{2+}, Al^{3+}, Co^{2+}, Ni^{2+}, Pd^{2+}, Cd^{2+}, Hg^{2+}, Cu^{2+}, Ba^{2+} , Pb^{2+} and Al^{3+}) in THF-MeOH (v/v 1 : 1) (pH 7.2) is insignificant. Thus, the probe is selectively showing "turn-on" emission to Zn^{2+} under the identical experimental condition (Fig. 3)[31,32]. On incremental addition of Zn^{2+} to the solution of H_2L the fluorescence intensity increases and becomes saturated when reached at 1 : 1 molar ratio which results enhancement of quantum yield to 0.0819 (39-fold increment compared to ligand). The emission intensity of the mixture does not change on excess addition of Zn^{2+} (Fig. 4). The augmentation in fluorescence intensity for H_2L+Zn^{2+} may arise from the elimination of photoinduced electron transfer (PET) in free H_2L and chelation enhancement effect (CHEF) through the

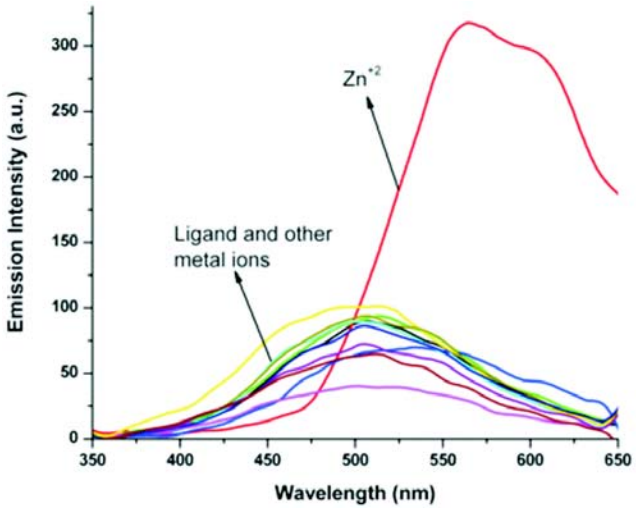

Fig. 3. Change in absorption spectrum of H_2L (50 μM) upon gradual addition of different metal ions (100 μM each) in THF-MeOH (v/v 1 : 1) (pH 7.2).

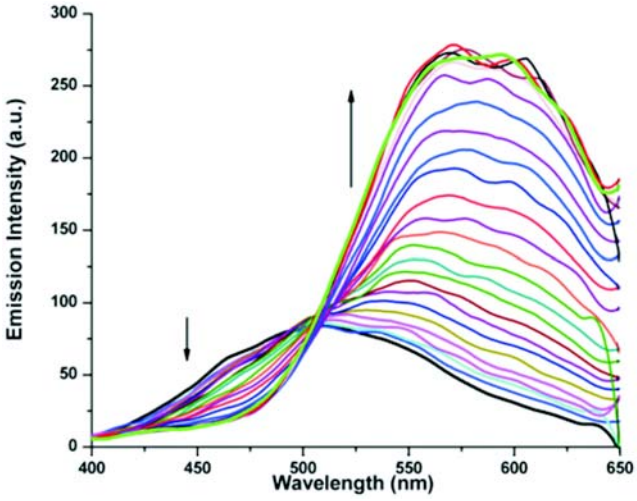

Fig. 4. Change in emission spectrum of H_2L (50 μM) upon gradual addition of Zn^{2+} ions (5 μM each) THF-MeOH (v/v 1 : 1) (pH 7.2).

co-ordination of imidazolyl-N, azomethine-N and hydrazide-O to metal ion (Scheme 1). To get further insight about the complexation reaction the fluorimetric titration has been done and $[(F_{max} - F_0)/(F - F_0)]$ vs $1/[Zn^{2+}]$ has been plotted following Benesi-Hildebrand equation (Fig. 5) and has determined the binding constant [K_d, 7.6×10^4]. The limit of detection (LOD) of Zn^{2+} has been calculated 0.36 μM following the 3σ method (ESI†, Fig. S5). The fluores-

cence enhancement of H_2L-Zn^{2+} complex has been examined in presence of other metal ions (Fig. 6).

Quinoline substituted fluorogenic motives[15,23] have been used in large number in the identification of different cations and anions; and the detection of Zn^{2+} appears in highest account. Some of the literature reports (Table 1) are selected considering structural similarity of present chemosensor; but quinoline-hydrazide is first time reported herewith.

Effect of pH variation on fluorescence intensity of H_2L and H_2L-Zn^{2+} complex has been studied; it has observed that there is no significant fluorescence emission of H_2L at the pH range 2 to 12 and in presence of Zn^{2+} the ligand emits in the pH range between 3.0 to 11 (Fig. 7). At high acidic medium (pH 2) ligand may be protonated or hydrolyse Schiff base while in the basic medium (pH 12) may precipitate $Zn(OH)_2$ and thus, inhibits the complexation. This indicates that H_2L is useful for detection of Zn^{2+} in the biological pH that is at much lower concentration than that of WHO recommended value (76 μM) in drinking water[33].

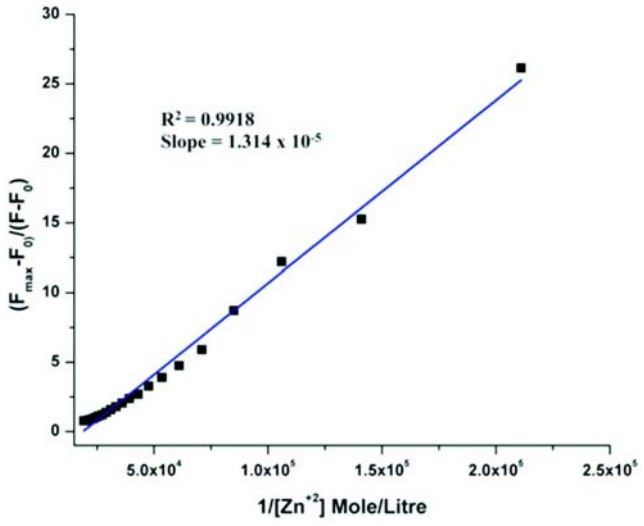

Fig. 5. Benesi-Hildebrand plot of $\{(F_{max} - F_o)/(F - F_o)\}$ vs $1/[Zn^{2+}]$ by fluorescence spectroscopy.

Lifetime data were obtained upon excitation at 450 nm, and the fluorescence decay curve was deconvoluted with respect to the lamp profile. The observed florescence decay fits nicely with the bi-exponential decay profile for both H_2L and complex (Fig. 8), which is supported by goodness of fit (χ^2) data in the regression analyses. The average lifetime value of [H_2L-Zn^{2+}] (0.5 ns) is longer than that of H_2L (0.038 ns). The metal-ligand orbital mixing in [H_2L-Zn^{2+}] may be the reason for the longer lifetime of the excited state.

Density functional theory calculation

Geometry optimization of H_2L and [$ZnL(H_2O)$] has been performed using DFT calculation with B3LYP method. The DFT optimized structure of the complex is a distorted tetrahedral where H_2L acts as O,N,N chelator to Zn^{2+}. The calculated Zn-N (imine), Zn-O (amide carbonyl) and Zn-N (imidazolium-N) distances are 2.04, 2.08 and 2.02 Å respectively and have been comparable with similar structure[31,32]. Upon coordination of metal ion with the H_2L, the energy of HOMO increased relative to those of free H_2L while LUMO decreases its energy relative to those of free H_2L. The decrease in the LUMO level is more significant indicating that the LUMO was more stabilized than the

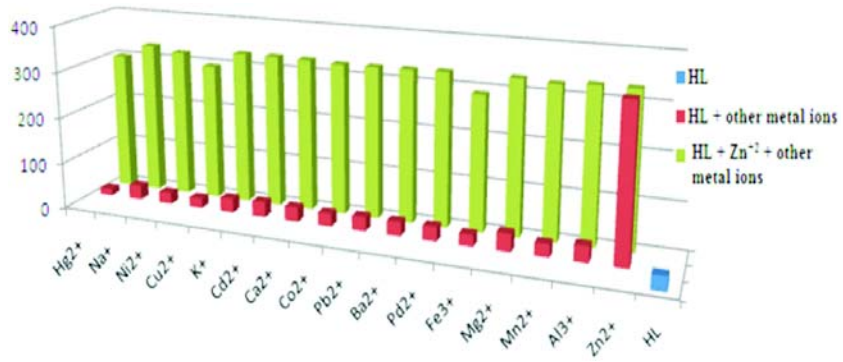

Fig. 6. Bar chart presenting fluorescence response of H_2L in presence of different metal ions.

Table 1. Structure of quinolinyl fluorophore, LOD of Zn^{2+} (and Reference)

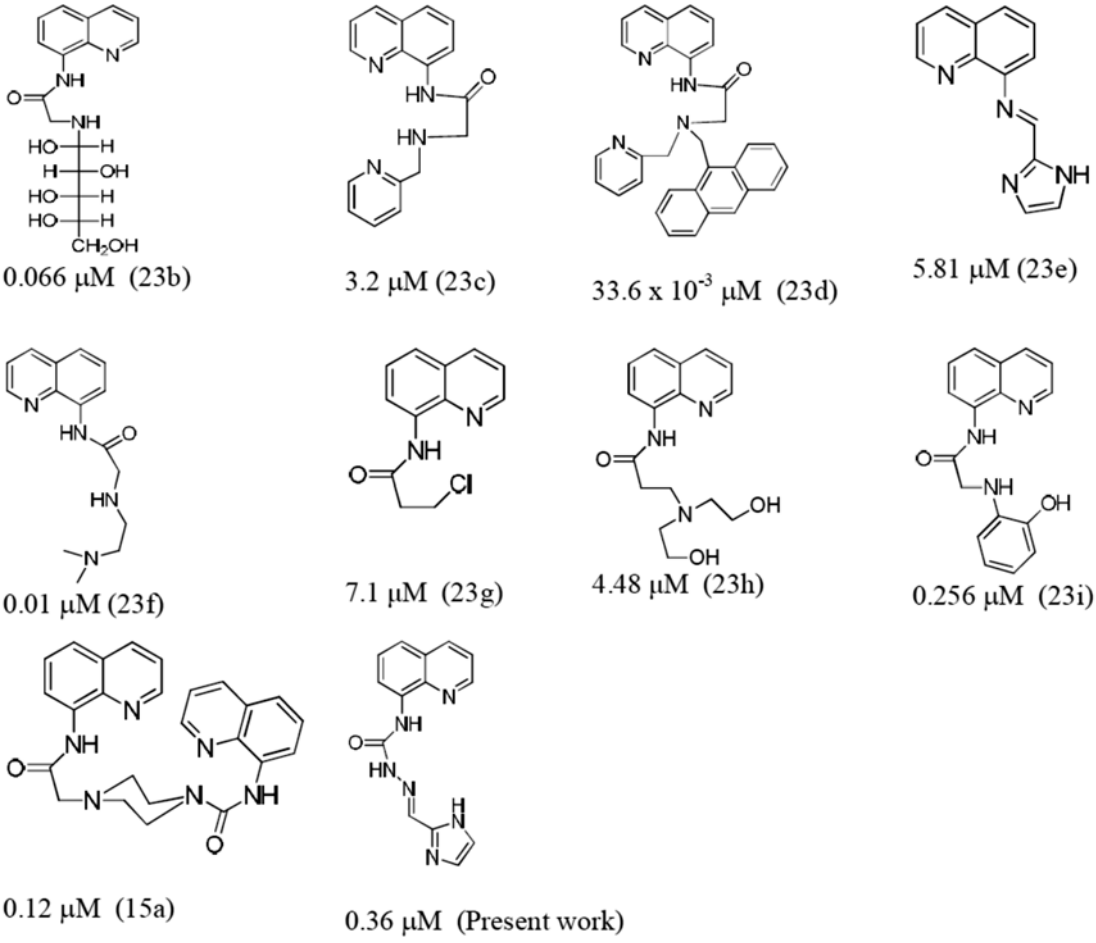

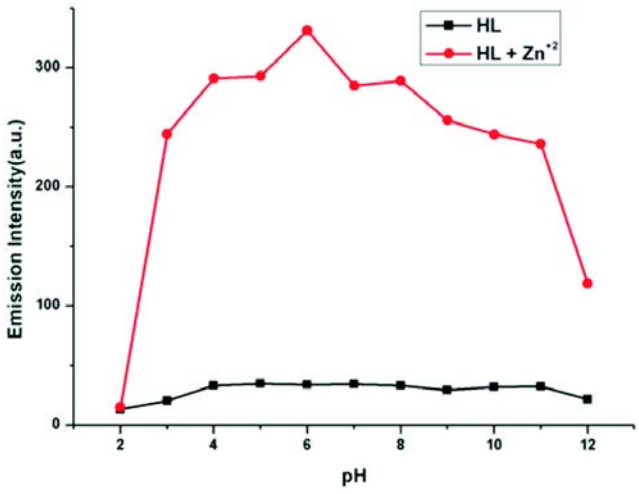

Fig. 7. Effect of pH on fluorescence intensity of receptor H_2L and H_2L-Zn^{2+} complex.

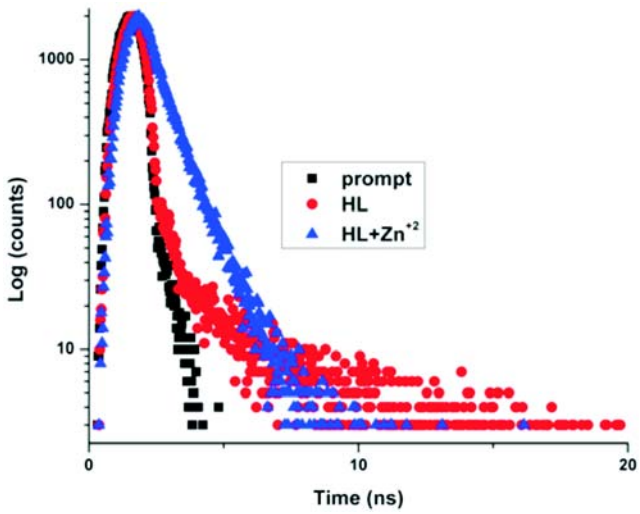

Fig. 8. Decay profile of H_2L and [H_2L-Zn^{2+}] complex.

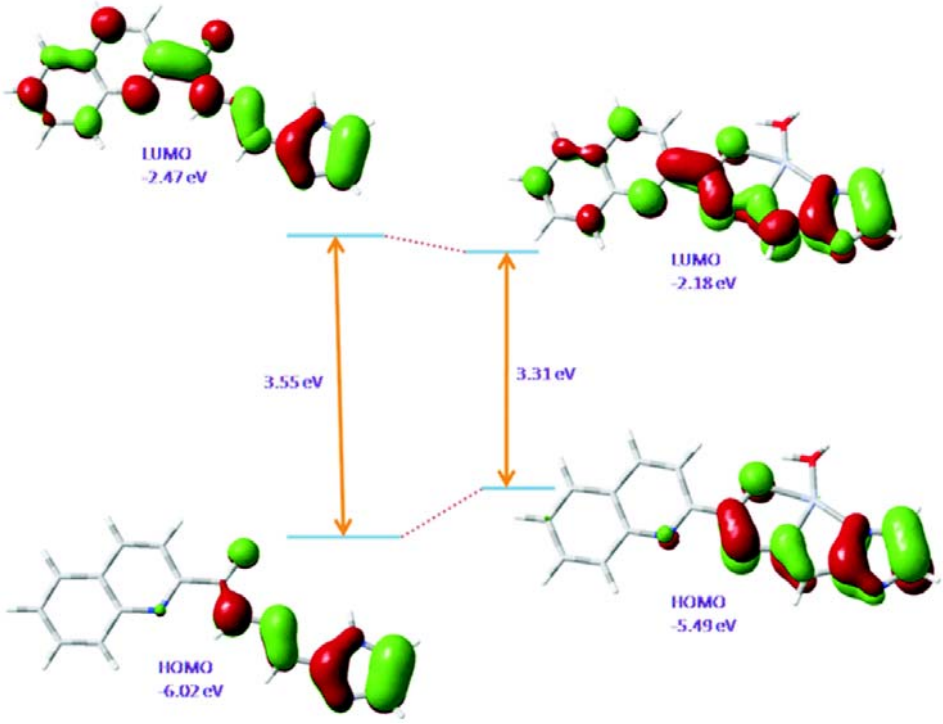

Fig. 9. Frontier molecular orbital of HL and $ZnL(H_2O)$.

HOMO. The HOMO-LUMO gap in H_2L (3.55 eV) has been decreased in $[ZnL(H_2O)]$ (3.31 eV) which supports the red shift of absorption band from 332 nm to 483 nm in UV-Vis spectra (Fig. 9).

Conclusion

Quinoline-hydrazide (H_2L) has been successfully used as "turn-on" fluorescence chemosensor to Zn^{2+} ion in presence of large number of other metal ions upon irradiation at 331 nm and shows high intense emission (λ_{em}, 575 nm). The limit of detection (LOD) for Zn^{2+} is 0.36 mM which is far below the WHO recommended limit (76 μM). The 1 : 1 metal-to-ligand complex has been ascertained by Mass spectra and Job's plot.

Acknowledgement

Financial support from the Council of Scientific and Industrial Research (CSIR, Sanction no. 01(2894)/09/EMR-II), New Delhi, India is gratefully acknowledged. One of the authors (RP) is thankful to Department of Science and Technology (DST), Govt. of India for providing DST-INSPIRE research fellowship.

References

1. I. Kienlen, *Ann Anesthesiol Fr.*, 1977, **18**, 1019.
2. I. Bertini, H. B. Gray, S. J. Lippard and J. S. Valentine, "Bioinorganic Chemistry", University Science Books, Mill Valley, California, 1994.
3. (a) "Zinc in Human Biology", ed. C. F. Mills, Springer-Verlag, Berlin, 1989; (b) J. C. King and R. J. Cousins, "Zinc, in Modern Nutrition in Health and Disease", eds. M. E. Shils, M. Shike, A. C. Ross, B. Caballero and R. J. Cousins, Lippincott Williams and Wilkins, Baltimore, 10th ed., 2006, 271.
4. (a) A. I. Bush, *Trends Neurosci.,* 2003, **26**, 207; (b) D. Noy, I. Solomonov, O. Sinkevich, T. Arad, K. Kjaer and I. Sagi, *J. Am. Chem. Soc.,* 2008, **130**, 1376.
5. A. Baran, *Pol. J. Environ. Stud.*, 2013, **22**, 77.
6. L. Li, F. Liu and H. W. Li, *Spectrochim. Acta, Part A*, 2011, **79**, 1688.
7. Y. Zhou, J. Yao, M. M. F. Choi, Y. J. Chen, H. Y. Chen, R. Mohammad, R. S. Zhuang, H. L. Chen, F. Wang, T. Maskow and G. Zaray, *J. Hazard. Mater.*, 2009, **169**, 875.
8. C. Patra, A. K. Bhanja, C. Sen, D. Ojha, D. Chattopadhyay, A. Mahapatra and C. Sinha, *Sens. Actuators (B)*, 2016, **228**, 287.
9. S. Goswami, A. Manna, S. Paul, A. K. Das, K. Aich and P. K. Nandi, *Chem. Commun.,* 2013, **49**, 2912.

10. S. Goswami, A. Manna, S. Paul, A. K. Das, P. K. Nandi, A. K. Maity and P. Saha, *Tetrahedron Lett.*, 2014, **55**, 490.

11. S. Goswami, A. K. Das, A. Manna, A. K. Maity, H. K. Fun, C. K. Quah and P. Saha, *Tetrahedron Lett.,* 2014, **55**, 2633.

12. J. S. Wu, W. M. Liu, J. C. Ge, H. Y. Zhang and P. F. Wang, *Chem. Soc. Rev.*, 2011, **40**, 3483.

13. S. Goswami, A. Manna, M. Mondal and D. Sarkar, *RSC Adv.,* 2014, **4**, 62639.

14. A. Manna and S. Goswami, *New J. Chem.,* 2015, **39**, 4424.

15. (a) J. Jiang, H. Jiang, X. Tang, L. Yang, W. Dou, W. Liu, R. Fang and W. Liu, *Dalton Trans.,* 2011, **40**, 6367; (b) P. Li, X. Zhou, R. Huang, L. Yang, X. Tang, W. Dou, Q. Zhao and W. Liu, *Dalton Trans.*, 2014, **43**, 706; (c) Q.-H. You, P.-S. Chan, W.-H. Chan, S. C. K. Hau, A. W. M. Lee, N. K. Mak, T. C. W. Makc and R. N. S. Wong, *RSC Adv.*, 2012, **2**, 11078.

16. (a) A. Ajayaghosh, P. Carol and S. Sreejith, *J. Am. Chem. Soc.*, 2005, **127**, 14962; (b) Y. Liu, Q. Fei, H. Shan, M. Cui, Q. Liu, G. Feng and Y. Huan, *Analyst*, 2014, **139**, 1868.

17. (a) D. Maity and T. Govindaraju, *Chem. Commun.*, 2012, **48**, 1039; (b) Z. Xu, X. Liu, J. Pan and D. R. Spring, *Chem. Commun.*, 2012, **48**, 4764.

18. (a) Z. Zhang, F.-W. Wang, S.-Q. Wang, F. Ge, B.-X. Zhao and J.-Y. Miao, *Org. Biomol. Chem.*, 2012, **10**, 8640; (b) A. Ciupa, M. F. Mahon, P. A. De Bank and L. Caggiano, *Org. Biomol. Chem.*, 2012, **10**, 8753.

19. Y. Ding, Y. Xie, X. Li, J. P. Hill, W. Zhang and W. Zhu, *Chem. Commun.*, 2011, **47**, 5431.

20. S.-Y. Jiao, L.-L. Peng, K. Li, Y.-M. Xie, M.-Z. Ao, X. Wang and X.-Q. Yu, *Analyst*, 2013, **138**, 5762.

21. (a) E. M. Nolan, S. C. Burdette, J. H. Harvey, S. A. Hilderbr and S. J. Lippard, *Inorg. Chem.*, 2004, **43**, 2624; (b) D. Wang, X. Xiang, X. Yang, X. Wang, Y. Guo, W. Liu and W. Qin, *Sens. Actuators (B)*, 2014, **201**, 246.

22. (a) Z. Xu, J. Yoon and D. R. Spring, *Chem. Soc. Rev.,* 2010, **39**, 1996; (b) G. Sivaraman, T. Anand and D. Chellappa, *Analyst,* 2012, **137**, 5881.

23. (a) Q.-J. Ma, X.-B. Zhang, Z.-X. Han, B. Huang, Q. Jiang, G.-L. Shen and R.-Q. Yu, *Int. J. Env. Anal. Chem.,* 2011, **91**, 74; (b) X.-B. Li, J.-Y. Chen, Z.-G. Niu and E.-J. Wang, *Indian J. Chem.*, 2014, **53A**, 1349 and references therein; (c) Y. Ma, F. Wang, S. Kambam and X. Chen, *Sens. Actuators (B)*, 2013, **188**, 1116; (d) Y. Ma. H. Chen, F. Wang, S. Kambam, Y. Wang, C. Mao and X. Chen, *Dyes and Pigments,* 2014, **102**, 301; (e) S. Mukherjee and S. Talukder, *J. Lumin.*, 2016, **177**, 40 and references therein; (f) G. J. Park, J. J. Lee, G. R. Youa, L. T. Nguyen, I. Noh and C. Kima, *Sens. Actuators (B)*, 2016, **223**, 509; (g) Y. S. Kim, J. J. Lee, S. Y. Lee, P.-G. Kim and C. Kim, *J. Fluoresc.*, 2016, **26**, 835; (h) Y. W. Choi, J. J. Lee and C. Kim, *RSC Adv.*, 2015, **5**, 60796; (i) Y. Yue, Q. Dong, Y. Zhang, Y. Sun and Y. Gong *Anal. Methods*, 2015, **7**, 5661.

24. B. K. Datta, D. Thiyagarajan, A. Ramesh and G. Das, *Dalton Trans.*, 2015, **44**, 13093.

25. J. Q. Umberger and V. K. LaMer, *J. Am. Chem. Soc.,* 1945, **67**, 1099.

26. M. J. Frisch, G. W. Trucks, H. B. Schlegel, G. E. Scuseria, M. A. Robb, J. R. Cheeseman, G. Scalmani, V. Barone, B. Mennucci, G. A. Petersson, H. Nakatsuji, M. Caricato, X. Li, H. P. Hratchian, A. F. Izmaylov, J. Bloino, G. Zheng, J. L. Sonnenberg, M. Hada, M. Ehara, K. Toyota, R. Fukuda, J. Hasegawa, M. Ishida, T. Nakajima, Y. Honda, O. Kitao, H. Nakai, T. Vreven, J. A. Montgomery (Jr.), J. E. Peralta, F. Ogliaro, M. Bearpark, J. J. Heyd, E. Brothers, K. N. Kudin, V. N. Staroverov, R. Kobayashi, J. Normand, K. Raghavachari, A. Rendell, J. C. Burant, S. S. Iyengar, J. Tomasi, M. Cossi, N. Rega, J. M. Millam, M. Klene, J. E. Knox, J. B. Cross, V. Bakken, C. Adamo, J. Jaramillo, R. Gomperts, R. E. Stratmann, O. Yazyev, A. J. Austin, R. Cammi, C. Pomelli, J. W. Ochterski, R. L. Martin, K. Morokuma, V. G. Zakrzewski, G. A. Voth, P. Salvador, J. J. Dannenberg, S. Dapprich, A. D. Daniels, O. Farkas, J. B. Foresman, J. V. Ortiz, J. Cioslowski and D. J. Fox, Gaussian 09, Revision D.01, Gaussian Inc, Wallingford, CT, 2009.

27. A. D. Becke, *J. Chem. Phys.*, 1993, **98**, 5648.

28. C. Lee, W. Yang and R. G. Parr, *Phys. Rev. (B)*, 1988, **37**, 785.

29. M. Cossi, N. Rega, G. Scalmani and V. Barone, *J. Comput. Chem.*, 2003, **24**, 669.

30. N. M. O'Boyle, A. L. Tenderholt and K. M. Langner, *J. Comput. Chem.*, 2008, **29**, 839.

31. A. K. Bhanja, C. Patra, S. Mondal, D. Ojha, D. Chattopadhyay and C. Sinha, *RSC Adv.*, 2015, **5**, 48997.

32. C. Patra, A. K. Bhanja, C. Sen, D. Ojha, D. Chattopadhyay and C. Sinha, *RSC Adv.*, 2016, **6**, 53378.

33. Guidelines for drinking-water quality (2nd ed.), Vol. 2. Health criteria and other supporting information. World Health Organization, Geneva, 1996.